IAC–2019–C1.2.11

Trajectory Design of the Lucy Mission to Explore the Diversity of the Jupiter Trojans

Jacob A. Englander
Aerospace Engineer, Navigation and Mission Design Branch, NASA Goddard Space Flight Center

Kevin Berry
Lucy Flight Dynamics Lead, Navigation and Mission Design Branch, NASA Goddard Space Flight Center

Brian Sutter
Totally Awesome Trajectory Genius, Lockheed Martin Space Systems, Littleton, CO

Dale Stanbridge
Lucy Navigation Team Chief, KinetX Aerospace, Simi Valley, CA

Donald H. Ellison
Aerospace Engineer, Navigation and Mission Design Branch, NASA Goddard Space Flight Center

Ken Williams
Flight Director, Space Navigation and Flight Dynamics Practice, KinetX Aerospace, Simi Valley, California

James McAdams
Aerospace Engineer, Space Navigation and Flight Dynamics Practice, KinetX Aerospace, Simi Valley, California

Jeremy M. Knittel
Aerospace Engineer, Space Navigation and Flight Dynamics Practice, KinetX Aerospace, Simi Valley, California

Chelsea Welch
Fantastically Awesome Deputy Trajectory Genius, Lockheed Martin Space Systems, Littleton, CO

Hal Levison
Principle Investigator, Lucy mission, Southwest Research Institute, Boulder, CO

Lucy, NASA's next Discovery-class mission, will explore the diversity of the Jupiter Trojan asteroids. The Jupiter Trojans are thought to be remnants of the early solar system that were scattered inward when the gas giants migrated to their current positions as described in the Nice model. There are two stable subpopulations, or "swarms," captured at the Sun-Jupiter L4 and L5 regions. These objects are the most accessible samples of what the outer solar system may have originally looked like. Lucy will launch in 2021 and will visit five Trojans, including one binary system. This paper discusses the target selection process, including a description of "alternate Lucys" that were ultimately passed over in favor of the final design. The mathematics of the trajectory optimization are also discussed.

I. Introduction

Lucy, recently selected as NASA's 13th Discovery-class mission, will perform flybys of five bodies in the Sun-Jupiter L4 and L5 Trojan swarms and one main-belt object. Lucy's targets include the C-type object 3548 Eurybates, the P-type objects 15094 Polymele and 617 Patroclus-Menoetius, the D-type objects 11351 Leucus and 21900 Orus, and the main-belt object 52246 Donaldjohanson. These objects span both the spectral and size diversity of the Jupiter Trojans. Lucy achieves this by using Earth flybys to enter into two consecutive elliptical orbits about the sun, which naturally pass through both both Sun-Jupiter L4 and L5 and small maneuvers are inserted to target our chosen Trojans.

This work addresses the Lucy trajectory as a member of a general class of missions known as "science cyclers," in which the spacecraft is placed onto an

orbit that alternates between a region where interesting bodies are found and some large body, in this case the Earth, whose gravity may be used to adjust the orbit at one apse. Science cycler trajectories allow a modest spacecraft to perform flybys of many bodies that might otherwise be difficult to reach, while requiring relatively little propellant compared to a rendezvous mission. Lucy is a member of a subclass of science cyclers called "Jupiter Trojan cyclers," so named because of the particular class of object being targeted. Trojan cyclers are especially interesting for several reasons. First, there is no other way to visit multiple Trojans without a much larger propulsion system. Second, it is very convenient that the period of an orbit that touches the Earth and passes through the Trojan swarms is both an integer multiple of the Earth's orbital period and exactly half of the Trojans' periods, making the Earth available to adjust the trajectory on each orbit and target particular bodies in each swarm. Third, it is easy to enter into a Trojan cycler orbit using Earth flybys and modest propulsion.

II. Physics Model

II.i Multiple Gravity Assist with n Deep-Space Maneuvers

The trajectory transcription used in this work is Evolutionary Mission Trajectory Generator (EMTG)'s Multiple Gravity Assist with n Deep-Space Maneuvers using Shooting (MGAnDSMs).[1,2] This transcription can model a trajectory with any number of impulsive maneuvers. MGAnDSMs models the trajectory between two boundary points as a two-point shooting phase. The trajectory is propagated forward in time from the left-hand boundary condition and backward in time from the right-hand boundary condition. The optimizer chooses the time of flight (TOF) for the phase, along with necessary parameters to define the magnitude and direction of any impulsive deep-space maneuver (DSM)s. The TOF from the left-hand boundary to the first DSM, as well as from each DSM to the next DSM or to the right-hand boundary where appropriate, is expressed as the product of a "burn index" η_i with the phase TOF. The sum of the η_i must equal 1.0, guaranteeing that the propagation arcs fit within the phase TOF. Therefore, if a phase has only one impulse, then the time from the left boundary to the DSM, Δt_1, and the time from the DSM to the right boundary, Δt_2 will be:

$$\Delta t_1 = \eta_1 TOF \quad [1]$$

$$\Delta t_2 = \eta_2 TOF \quad [2]$$

Mass is propagated across each impulse by means of the exponential form of the rocket equation as shown in Equation 3.

$$m_i^+ = m_i^- \exp\left(\frac{-\Delta v}{I_{sp} g_0}\right) \quad [3]$$

where m_i^- is the mass of the spacecraft before the maneuver, m_i^+ is the mass of the spacecraft after the maneuver, Δv is the magnitude of the impulsive DSM, g_0 is the acceleration due to gravity at sea level on Earth, and I_{sp} is the specific impulse of the spacecraft's thruster.

The low-fidelity trajectories in this work are modeled using two-body dynamics and propagated by solving Kepler's problem. EMTG uses a universal-variable formulation, combined with a variable-order Laguerre root finder.[3,4]

Once the broad search of trajectories is complete, EMTG can also optimize high-fidelity trajectories using an 8th-order fixed-step Runge-Kutta explicit integrator,[6] n-body point mass gravity, the J_2 term of the central body, and solar radiation pressure. A fixed step integrator is used to ensure that the analytical partial derivatives of the final state with respect to the initial state and the time of integration are exact.[7]

II.ii Launch

In low fidelity, EMTG uses a patched-conic, zero-sphere of influence (SOI) approximation of launch. The optimizer chooses the launch epoch and the outgoing v_∞, Right Ascension of Launch Asymptote (RLA), and Declination of Launch Asymptote (DLA). The patched-conic launch model does not add any constraints to the problem. The initial state of the spacecraft in the heliocentric reference frame is then computed at the center of the launch body as per Equations 4-11. The coefficients in Equation 11 are a polynomial fit to the performance of the actual launch vehicle, which in the case of Lucy is an Atlas V 401.

$$C_3 = v_\infty^2 \quad [4]$$
$$x_0 = x_{body}\left(t_{launch}\right) \quad [5]$$
$$y_0 = y_{body}\left(t_{launch}\right) \quad [6]$$
$$z_0 = z_{body}\left(t_{launch}\right) \quad [7]$$
$$\dot{x}_0 = \dot{x}_{body}\left(t_{launch}\right) + C_3 \cos RLA \cos DLA \quad [8]$$
$$\dot{y}_0 = \dot{y}_{body}\left(t_{launch}\right) + C_3 \sin RLA \cos DLA \quad [9]$$
$$\dot{z}_0 = \dot{z}_{body}\left(t_{launch}\right) + C_3 \sin DLA \quad [10]$$
$$m_0 = a_{LV} + b_{LV}C_3 + c_{LV}C_3^2 + d_{LV}C_3^3 + e_{LV}C_3^4 + f_{LV}C_3^5 \quad [11]$$

When EMTG is used to optimize Lucy in high fidelity, the launch is modeled by an impulsive departure from a circular parking orbit at 185 km altitude. EMTG then propagates from the departure maneuver to the point at which Lucy exits the SOI of the Earth. This technique is fully described by Ellison *et al.*[8]

II.iii Gravity Assist Model

EMTG uses two different models for Lucy's Earth gravity assists, depending on the fidelity of the simulation. In low fidelity, EMTG uses a patched-conic, zero-SOI approximation that is common to many preliminary design tools. This is done by adding six new decision variables, defining the incoming and outgoing $\mathbf{v}_\infty$, and two new constraints: one to require that the magnitude of $v_{\infty,out}$ matches the magnitude of $v_{\infty,in}$, and one to ensure that the bend angle does not require the spacecraft to fly below a user-defined safe distance h_{safe} from the body, as described in Equations 12-14, where F is the constraint posed to the optimizer. In the context of Lucy, h_{safe} is 300 km. The flyby is un-powered, *i.e.*, no maneuver occurs at periapse.

$$F = h_{FB} - h_{safe} \quad [12]$$
$$h_{FB} = \frac{\mu}{v_{\infty,out}^2}\left(\frac{1}{\sin\frac{\delta_{FB}}{2}} - 1\right) - r_{body} \quad [13]$$
$$\delta_{FB} = \arccos\left(\frac{\mathbf{v}_{\infty,out} \bullet \mathbf{v}_{\infty,in}}{v_{\infty,out}v_{\infty,in}}\right) \quad [14]$$

When EMTG is used to optimize Lucy in high fidelity, the gravity assist maneuvers are modeled by propagating through the finite SOI of the Earth, with the Earth as the central body. This technique is fully described by Ellison *et al.*[8]

II.iv Encounter Model

EMTG models the Trojan and Donaldjohanson encounters as an intercept, *i.e*, a match of the precise position of the body but with a non-zero $\mathbf{v}_\infty$ vector. Since the Trojans and Donaldjohanson are very small, EMTG does not model a bend angle. This model is used in both low-fidelity and high-fidelity trajectory optimization, as it is adequate to provide an initial guess for a flight navigation tool.

III. Solver

III.i Nonlinear Programming

The optimization of the MGAnDSMs problems in this work may be formulated as nonlinear program (NLP) problems. The optimizer solves a problem of the form:

$$\begin{aligned} &\text{Minimize } f(\mathbf{x}) \\ &\text{Subject to:} \\ &\mathbf{x}_{lb} \le \mathbf{x} \le \mathbf{x}_{ub} \\ &\mathbf{c}(\mathbf{x}) \le \mathbf{0} \\ &A\mathbf{x} \le \mathbf{0} \end{aligned} \quad [15]$$

where $\mathbf{x}_{lb}$ and $\mathbf{x}_{ub}$ are the lower and upper bounds on the decision vector, $\mathbf{c}(\mathbf{x})$ is a vector of nonlinear constraint functions, and A is a matrix describing any linear constraints (*e.g.* time constraints).

The problems in this work, like most other interplanetary trajectory optimization problems, consist of hundreds of variables and tens to hundreds of constraints. Such problems are best solved with a *sparse* NLP solver such as Sparse Nonlinear OPTimizer (SNOPT).[9] SNOPT uses a sparse sequential quadratic programming (SQP) method and benefits greatly from precise knowledge of the problem Jacobian, *i.e.*, the matrix of partial derivatives of the objective function and constraints with respect to the decision variables. EMTG provides analytical expressions for all of the necessary partial derivatives, leading to improved convergence *vs.* using numerically approximated derivatives.[2,10,11] SNOPT, like all NLP solvers, requires an initial guess of the solution and tends to converge to a solution in the neighborhood of that initial guess. The next section discusses EMTG's fully automated method for generating initial guesses.

III.ii Monotonic Basin Hopping

In the past two decades, researchers have explored stochastic search methods that do not require an initial guess. Stochastic search techniques allow an automated system to efficiently design a complex trajectory without human input.[1,12–22] EMTG is designed

to operate without user oversight, and so relies heavily upon stochastic search. The particular stochastic search method used in this work is monotonic basin hopping (MBH).

MBH[23] is an algorithm for searching for the best solutions to problems with many local optima. Many problems, including those described in this work, are structured such that individual locally optimal "basins" cluster together, where the distance in the decision space from one local optima to the next in a given cluster may be traversed in a short "hop." A problem may have several such clusters. MBH was originally developed to solve molecular conformation problems in computational chemistry, but has been demonstrated to be effective on various types of interplanetary trajectory problems.[12,18–20,24,25] Pseudocode for MBH is given in Algorithm 1.

Special attention is given to decision variables that define the time-of-flight between two boundary points, *e.g.* Earth or Trojan flybys in Lucy. These are the most significant variables that define a trajectory and therefore it is sometimes necessary to drastically perturb them in order to "hop" to a new cluster of solutions. With some (low) uniform-random probability ρ, each time-of-flight variables is shifted by $\pm$ 1 synodic period of the two boundary points defining that trajectory phase. In preliminary design for Lucy, ρ was set to 0.05. In high fidelity re-optimization, ρ is set to 0.0, because we do not expect significant changes to the trajectory.

MBH is run until either a specified number of iterations (trial points attempted) or a maximum CPU time is reached, at which point the best solution stored in the archive is returned. The version of MBH used in EMTG has two parameters: the stopping criterion and the type of random step used to generate the perturbed decision vector $\mathbf{x}'$. In this work, the random step is drawn from a bi-directional Pareto distribution with the Pareto parameter, α, set to 1.4. The bi-directional Pareto distribution usually generates small steps that allow MBH to *exploit* the local cluster around the current best solution. However, some of the steps generated by the bi-directional Pareto distribution are much larger, in some cases spanning the entire decision space. These larger steps allow MBH to *explore* the full decision space. This approach has been shown to be robust on complex interplanetary trajectory design problems.[22]

Algorithm 1 Monotonic Basin Hopping (MBH)

generate random point $\mathbf{x}$
run NLP solver to find point $\mathbf{x}^*$ using initial guess $\mathbf{x}$
$\mathbf{x}_{current} = \mathbf{x}^*$
if $\mathbf{x}^*$ is a feasible point **then**
  save $\mathbf{x}^*$ to archive
end if
while not hit stop criterion **do**
  generate $\mathbf{x}'$ by randomly perturbing $\mathbf{x}_{current}$
  for each time-of-flight variable t_i in $\mathbf{x}'$ **do**
    if $rand\,(0,1) < \rho_{time-hop}$ **then**
      shift t_i forward or backward one synodic period
    end if
  end for
  run NLP solver to find locally optimal point $\mathbf{x}^*$ using in initial guess $\mathbf{x}'$
  if $\mathbf{x}^*$ is feasible **and** $f(\mathbf{x}^*) < f(\mathbf{x}_{current})$ **then**
    $\mathbf{x}_{current} = \mathbf{x}^*$
    save $\mathbf{x}^*$ to archive
  else if $\mathbf{x}^*$ is infeasible **and** $\|c(\mathbf{x}^*)\| < \|c(\mathbf{x}_{current})\|$)
    $\mathbf{x}_{current} = \mathbf{x}^*$
  end if
end while
return best $\mathbf{x}^*$ in archive

IV. Baseline Lucy

The computational process described in the previous section is successfully applied to the Lucy mis-

sion. Lucy includes a launch, three Earth gravity assists, six small-body encounters, and nine MGAnDSMs phases. Figure 1 shows the problem structure as defined in EMTG.

The Lucy trajectory presented here, as developed for critical design review (CDR), was optimized first in EMTG's low-fidelity mode with Kepler propagation and patched-conic gravity assists, and then in EMTG's high-fidelity mode with numerical integration, n-body gravity, Sample Return Capsule (SRC) and fully modeled gravity assists. The objective function is to maximize dry mass. The low-fidelity solution was used as a starting point for the high-fidelity optimization. Table 1 is a comparison of the low-fidelity and high-fidelity trajectories. Note that the low-fidelity, patched conic run yields a lower Δv, and higher dry mass, than the high-fidelity run because the low-fidelity run does not account for solar radiation pressure (SRP) or n-body perturbations.

Figures 2 and 3 show the trajectory in an ecliptic plane projection and in a side view, respectively. From Figure 3, it is clear that Lucy's Trojan asteroid targets lie in significantly different orbital planes. The Lucy mission is only possible because each of these targets cross the ecliptic plane in approximately the same place.

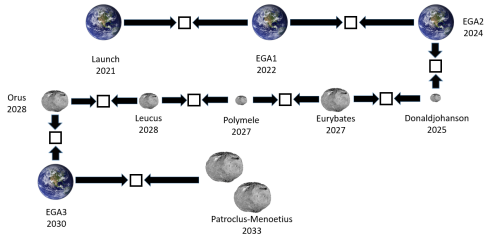

Fig. 1: Structure of the Lucy mission

V. Alternate Lucy

The Lucy trajectory has a family of near-cousins that visit the same three "large" Jupiter Trojan targets—3548 Eurybates, 21900 Orus, and 617 Patroclus-Menoetius. Each member of the Lucy family may visit a different set of smaller targets, depending on what is convenient. Lucy's targets are all available in the same mission because they all cross the ecliptic plane in the same place, that is, they share the same right ascension of the ascending node, Ω, $+/-180°$. The $+/-180°$ is included because for the purpose of a flyby cycler, it is not important whether the body is at its ascending or descending node at a

Table 1: Comparison of the low- and high-fidelity EMTG Lucy trajectories, for the October 16th, 2021 launch opportunity.

Parameter	EMTG (low-fidelity)	EMTG (high-fidelity)
Launch	10/16/2021	10/16/2021
DSM1 epoch	4/23/2022	11/15/2021
DSM1	2.1 m/s	3.8 m/s
EGA1 epoch	10/17/2022	10/16/2022
EGA1 altitude	300 km	300 km
DSM2 epoch	2/1/2024	2/7/2024
DSM2	889.6 m/s	910.9 m/s
EGA2 epoch	12/13/2024	12/13/2024
EGA2 altitude	341 km	334 km
Donaldjohanson epoch	4/20/2025	4/20/2025
DSM3 epoch	4/13/2027	4/7/2027
DSM3 magnitude	308.6 m/s	312.9 m/s
Eurybates epoch	8/12/2027	8/12/2027
Polymele epoch	9/15/2027	9/15/2027
DSM4 epoch	9/29/2027	9/29/2027
DSM4 magnitude	114.7 m/s	115.9 m/s
Leucus epoch	4/18/2028	4/18/2028
DSM5 epoch	7/22/2028	7/23/2028
DSM5 magnitude	349.7 m/s	350.8 m/s
Orus epoch	11/11/2028	11/11/2028
EGA3 epoch	12/27/2030	12/27/2030
EGA3 altitude	654 km	611 km
Patroclus epoch	3/3/2033	3/3/2033
Total Δv	1664.7 m/s	1693.5 m/s

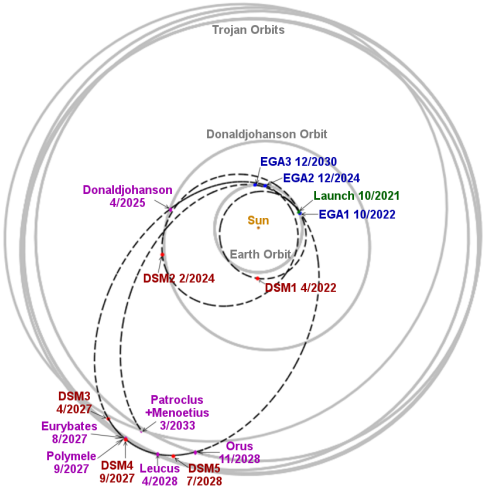

Fig. 2: Ecliptic-plane projection of the Lucy baseline trajectory

Table 2: Physical and Orbital Characteristics of Lucy's Targets

Body	H	Spectral Class	a (AU)	e	i	Ω	ω
52246 Donaldjohanson	15.5		2.38	0.19	4.4	262.9	213.0
3548 Eurybates	9.7	C	5.19	0.09	8.1	43.6	28.0
15094 Polymele	11.7	P	5.16	0.09	13.0	50.3	4.9
11351 Leucus	10.7	D	5.29	0.06	11.6	251.1	161.2
21900 Orus	10.0	D	5.13	0.04	8.5	258.6	180.5
617 Patroclus-Menoetius	8.2	P	5.22	0.14	22.0	44.4	308.4

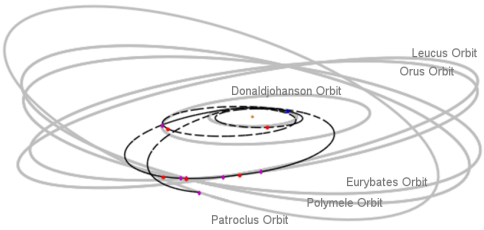

Fig. 3: Side view of the Lucy baseline trajectory

particular epoch as long as it is passing through the ecliptic plane.

Furthermore, Lucy's targets share a very similar argument of perihelion, ω, except for Leucus, which happens to have a very low eccentricity so ω is less important. Figure 4 shows ω vs mod $(\Omega, 180°)$ for all of the large Trojans for which a spectral class is known. 15094 Polymele and 11351 Leucus do not appear on this chart but have been recently classified as a P and D, respectively. Table 2 shows the physical and orbital characteristics of all of the Lucy targets. The Lucy target set is particularly exciting because it includes not only at least one of each spectral class, but also a small P and D in 15094 Polymele and 11351 Leucus, the parent body of the only known Jupiter Trojan collisional family in 3548 Eurybates, and an equal mass binary in 617 Patroclus-Menoetius. 617 Patroclus-Menoetius is of special interest because equal mass binaries are thought to be more common among the Kuiper Belt objects (KBOs).

The backup Lucy trajectory launches in 2022 and skips the first Earth flyby but is otherwise nearly identical to the nominal Lucy. A 2024 launch is also possible but does not include any Earth flybys and requires a large rocket to throw to a high C_3. These two options are shown in Figure 5.

However, the nominal and backup 2022 and 2024 high C_3 trajectories represent only one subfamily of the Lucy cycler family, which we call "Forward Lucy." The other half of the Lucy family of trajectories go to 617 Patroclus-Menoetius first and are known as

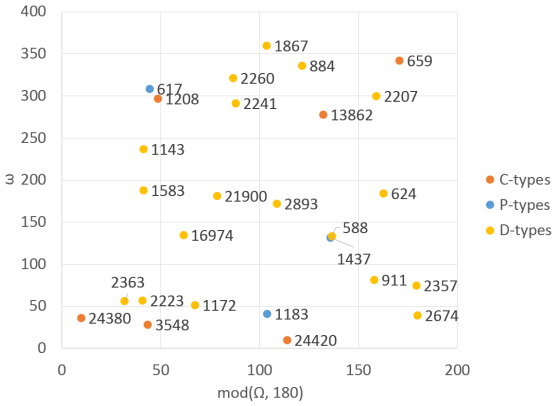

Fig. 4: ω vs mod $(\Omega, 180°)$ for all large classified Trojans—feasible Trojan science cyclers visit families of objects with similar ω and mod $(\Omega, 180°)$

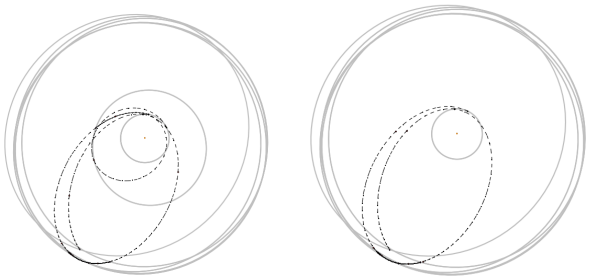

Fig. 5: Lucy 2022 (L) and 2024 high C_3 (R) trajectories

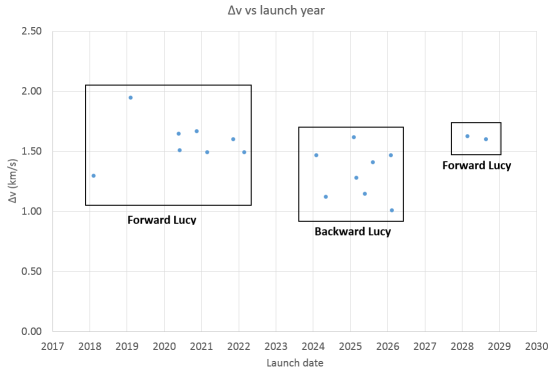

Fig. 6: Δv vs launch year for all low C_3 members of the Lucy cycler family

"Backward Lucy." The Backward Lucy trajectories become available starting in 2024 and are characterized by several Earth flybys and a long flight time. As the launch date moves forward each year, one can remove an Earth flyby or otherwise change the pump-up geometry and still access the Lucy targets in the backwards (617 Patroclus-Menoetius first) order. This pattern continues from 2024 to 2027, at which time it is no longer possible to launch to the Backward Lucy family.

The Forward Lucy family is once again available with a low C_3 launch in 2029. The required Δv remains in the 1.0-2.0 km/s range that the Lucy spacecraft can achieve. The pattern eventually falls apart because 21900 Orus has a slightly shorter period than 3548 Eurybates and 617 Patroclus-Menoetius and therefore gets too far "ahead" of them in its orbit and it is no longer possible to connect all three bodies. This same phenomenon causes 15094 Polymele and 11351 Leucus to be unavailable after the 2024 high C_3 opportunity.

Figure 6 shows the required Δv for each of the low C_3, *i.e.* below 40 km^2/s^2, members of the Lucy cycler family. Figure 7 shows the end date of the different sub-families of Lucy cyclers. Note that all of the first set of Forward Lucys end in the same month in 2033, all of the Backward Lucys end in 2040, and the second set of Forward Lucys end in 2044. In order for this to work, the flight time drops by one year for each later launch year as shown in Figure 8.

The Lucy cycler family is a special case of the general class of Jupiter Trojan cycler. Lucy-like trajectories are available for other sets of Jupiter Trojans, with the caveat that they must all share the same $mod\,(\Omega, 180°)$ and in most cases should share the same argument of perihelion (AOP). Other Trojan

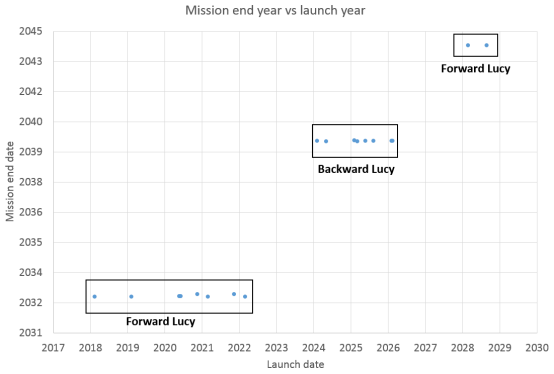

Fig. 7: Mission end date vs launch year for all low C_3 members of the Lucy cycler family

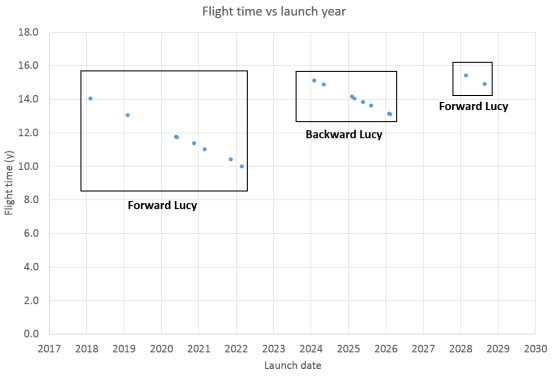

Fig. 8: Flight time vs launch year for all low C_3 members of the Lucy cycler family

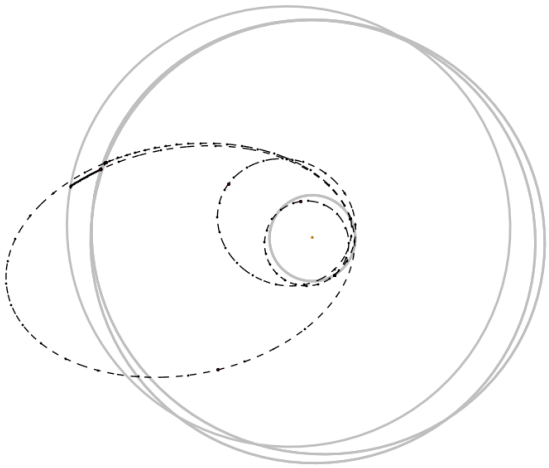

Fig. 9: An alternative Jupiter Trojan science cycler that visits 2207 Antenor, 624 Hektor, and 659 Nestor. This family of cyclers does not offer good science observation geometry and may freeze the spacecraft to death.

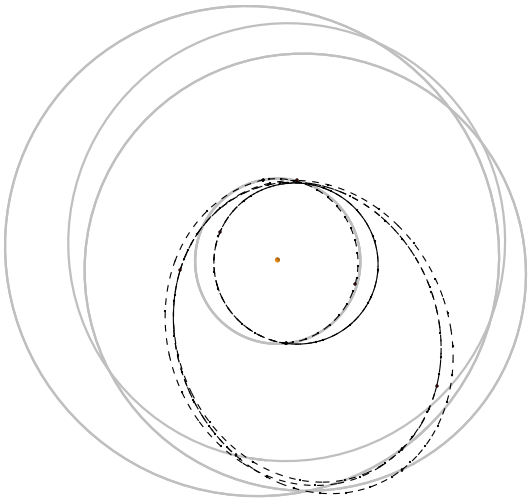

Fig. 10: A notional main-belt science cycler that visits 221 Eos, 114 Kassandra, and 26 Proserpina

cycler families have been found, including the trajectory that visits 2207 Antenor, 624 Hektor, and 659 Nestor as shown in Figure 9. However none of the other Jupiter Trojan cycler families that we found provided the science value of the Lucy family of trajectories. The Hektor-Nestor family of Trojan cyclers is also less appealing than the Lucy family because Hektor and Nestor have opposing perihelia - one is always at perihelion when the other is aphelion. It is therefore only possible to visit both of them in a single orbit by either approaching directly from sunward or diving down on them from a higher solar distance. In both cases the encounter velocities are very high and do not enable good science observations.

All Jupiter Trojan cyclers are in turn a special case of the general class of science flyby cyclers. Science flyby cycler trajectories can also be constructed to tour the main belt or of the Trojans associated with any of the other planets in the solar system, although there are not many of those known at the time of this writing. Figure 10 is a plot of a notional main-belt science cycler that visits 221 Eos, 114 Kassandra, and 26 Proserpina. Like Lucy and her immediate family, the main-belt science cyclers make use of the Earth's gravity and small chemical maneuvers to visit multiple targets.

VI. Conclusion

The direct transcription and nonlinear programming approach, when combined with the monotonic basin hopping global search heuristic as described in this work, proved to be a very effective method for optimizing the trajectory for Lucy and her Trojan-cycler cousins. Many multi-Trojan tours were found. The most compelling of these from a science value, mission length, and Δv perspective is the trajectory that Lucy will fly. The techniques described in this paper will be used by the Lucy flight dynamics team throughout the mission and to design future missions by Goddard Space Flight Center and KinetX Aerospace.

Acknowledgments

The authors would like to acknowledge the Lucy project for funding this work, as well as Goddard Space Flight Center's IRAD program for funding the development of EMTG. Jacob Englander would like to dedicate this paper to Howard Williams, who passed away in 2017 when we began writing this paper. We did not publish it then, and so it is fitting that we recognize him when publishing it now.

References

[1] M. Vavrina, J. Englander, and D. Ellison, "Global Optimization of N-Manuever, High-Thrust Trajectories Using Direct Multiple Shooting," *AAS/AIAA Space Flight Mechanics Meeting*, February 2016.

[2] D. H. Ellison, B. A. Conway, J. A. Englander, and M. T. Ozimek, "Application and Analysis of Bounded-Impulse Trajectory Models with Analytic Gradients," *Journal of Guidance, Control, and Dynamics*, Vol. 41, No. 8, 2018, pp. 1700–1714, 10.2514/1.G003078.

[3] J. Prussing and B. Conway, *Orbital Mechanics*. Oxford University Press, New York, 1993.

[4] G. J. Der, "Classical and Advanced Kepler Algorithms," `http://derastrodynamics.com/docs/kepler_algorithms_v2.pdf`.

[5] "SPICE Ephemeris," `http://naif.jpl.nasa.gov/naif/`, accessed 6/26/2016.

[6] P. Prince and J. Dormand, "High order embedded Runge-Kutta formulae," *Journal of Computational and Applied Mathematics*, Vol. 7, No. 1, 1981, pp. 67 – 75, https://doi.org/10.1016/0771-050X(81)90010-3.

[7] E. Pellegrini and R. Russell, "On the Computation and Accuracy of Trajectory State Transition Matrices," *Journal of Guidance, Control, and Dynamics*, Vol. 39, 09 2016, pp. 2485–2499, 10.2514/1.G001920.

[8] D. H. Ellison and J. A. Englander, "High-Fidelity Multiple-Flyby Trajectory Optimization Using Multiple Shooting," *AAS/AIAA Astrodynamics Specialist Conference*, 2019.

[9] P. E. Gill, W. Murray, and M. A. Saunders, "SNOPT: An SQP Algorithm for Large-Scale Constrained Optimization," *SIAM J. Optim.*, Vol. 12, jan 2002, pp. 979–1006, 10.1137/s1052623499350013.

[10] D. H. Ellison, B. A. Conway, J. A. Englander, and M. T. Ozimek, "Analytic Gradient Computation for Bounded-Impulse Trajectory Models Using Two-Sided Shooting," *Journal of Guidance, Control, and Dynamics*, Vol. 41, No. 7, 2018, pp. 1449–1462, 10.2514/1.G003077.

[11] D. H. Ellison, *Robust Preliminary Design for Multiple Gravity Assist Spacecraft Trajectories*. PhD thesis, May 2018.

[12] C. H. Yam, D. D. Lorenzo, and D. Izzo, "Low-thrust trajectory design as a constrained global optimization problem," Vol. 225, SAGE Publications, aug 2011, pp. 1243–1251, 10.1177/0954410011401686.

[13] G. A. Rauwolf and V. L. Coverstone-Carroll, "Near-optimal low-thrust orbit transfers generated by a genetic algorithm," *Journal of Spacecraft and Rockets*, Vol. 33, nov 1996, pp. 859–862, 10.2514/3.26850.

[14] V. Coverstone-Carroll, "Near-Optimal Low-Thrust Trajectories via Micro-Genetic Algorithms," *Journal of Guidance, Control, and Dynamics*, Vol. 20, jan 1997, pp. 196–198, 10.2514/2.4020.

[15] V. Coverstone-Carroll, J. Hartmann, and W. Mason, "Optimal multi-objective low-thrust spacecraft trajectories," *Computer Methods in Applied Mechanics and Engineering*, Vol. 186, jun 2000, pp. 387–402, 10.1016/s0045-7825(99)00393-x.

[16] M. Vavrina and K. Howell, "Global Low-Thrust Trajectory Optimization Through Hybridization of a Genetic Algorithm and a Direct Method," *AIAA/AAS Astrodynamics Specialist Conference and Exhibit*, AIAA, aug 2008, 10.2514/6.2008-6614.

[17] J. A. Englander, B. A. Conway, and T. Williams, "Automated Mission Planning via Evolutionary Algorithms," *Journal of Guidance, Control, and Dynamics*, Vol. 35, nov 2012, pp. 1878–1887, 10.2514/1.54101.

[18] J. A. Englander, B. A. Conway, and T. Williams, "Automated Interplanetary Mission Planning," *AAS/AIAA Astrodynamics Specialist Conference, Minneapolis, MN*, AIAA paper 2012-4517, August 2012, 10.2514/6.2012-4517.

[19] J. A. Englander, *Automated Trajectory Planning for Multiple-Flyby Interplanetary Missions*. PhD thesis, University of Illinois at Urbana-Champaign, April 2013.

[20] D. H. Ellison, J. A. Englander, and B. A. Conway, "Robust Global Optimzation of Low-Thrust, Multiple-Flyby Trajectories," *AAS/AIAA Astrodynamics Specialist Conference, Hilton Head, SC*, AAS paper 13-924, August 2013.

[21] D. H. Ellison, J. A. Englander, M. T. Ozimek, and B. A. Conway, "Analytical Partial Derivative Calculation of the Sims-Flanagan Transcription Match Point Constraints," *AAS/AIAA Space-Flight Mechanics Meeting, Santa Fe, NM*, AAS, January 2014.

[22] J. A. Englander and A. C. Englander, "Tuning Monotonic Basin Hopping: Improving the Efficiency of Stochastic Search as Applied to Low-Thrust Trajectory Optimization," *24th International Symposium on Space Flight Dynamics, Laurel, MD*, ISSFD, May 2014.

[23] R. H. Leary, "Global Optimization on Funneling Landscapes," *Journal of Global Optimization*, Vol. 18, No. 4, 2000, pp. 367–383, 10.1023/A:1026500301312.

[24] B. Addis, A. Cassioli, M. Locatelli, and F. Schoen, "A global optimization method for the design of space trajectories," *Computational Optimization and Applications*, Vol. 48, jun 2009, pp. 635–652, 10.1007/s10589-009-9261-6.

[25] J. Englander, M. A. Vavrina, B. J. Naasz, R. G. Merrill, and M. Qu, "Mars, Phobos, and Deimos Sample Return Enabled by ARRM Alternative Trade Study Spacecraft," *AIAA/AAS Astrodynamics Specialist Conference*, AIAA paper 2014-4354, aug 2014, 10.2514/6.2014-4354.

[26] J. Knittel, K. Hughes, J. Englander, and B. Sarli, "Automated Sensitivity Analysis of Interplanetary Trajectories for Optimal Mission Design," *International Symposium on Space Flight Dynamics, Matsuyama, Japan*, June 2017.